

**Review Article (Invited)****Activation mechanism of the bacterial flagellar dual-fuel protein export engine**Tohru Minamino<sup>1</sup>, Miki Kinoshita<sup>1</sup>, Yusuke V. Morimoto<sup>2,3</sup>, Keiichi Namba<sup>1,4,5</sup><sup>1</sup> Graduate school of Frontier Biosciences, Osaka University, Suita, Osaka 565-0871, Japan<sup>2</sup> Department of Physics and Information Technology, Faculty of Computer Science and Systems Engineering, Kyushu Institute of Technology, Izuka, Fukuoka 820-8502, Japan<sup>3</sup> Precursory Research for Embryonic Science and Technology, Japan Science and Technology Agency, Kawaguchi, Saitama 332-0012, Japan<sup>4</sup> RIKEN SPring-8 Center, Suita, Osaka 565-0871, Japan<sup>5</sup> JEOL YOKOGUSHI Research Alliance Laboratories, Osaka University, Suita, Osaka 565-0871, Japan

Received November 1, 2022; Accepted November 17, 2022;  
Released online in J-STAGE as advance publication November 19, 2022  
Edited by Haruki Nakamura

Bacteria employ the flagellar type III secretion system (fT3SS) to construct flagellum, which acts as a supramolecular motility machine. The fT3SS of *Salmonella enterica* serovar Typhimurium is composed of a transmembrane export gate complex and a cytoplasmic ATPase ring complex. The transmembrane export gate complex is fueled by proton motive force across the cytoplasmic membrane and is divided into four distinct functional parts: a dual-fuel export engine; a polypeptide channel; a membrane voltage sensor; and a docking platform. ATP hydrolysis by the cytoplasmic ATPase complex converts the export gate complex into a highly efficient proton (H<sup>+</sup>)/ protein antiporter that couples inward-directed H<sup>+</sup> flow with outward-directed protein export. When the ATPase ring complex does not work well in a given environment, the export gate complex will remain inactive. However, when the electric potential difference, which is defined as membrane voltage, rises above a certain threshold value, the export gate complex becomes an active H<sup>+</sup>/protein antiporter to a considerable degree, suggesting that the export gate complex has a voltage-gated activation mechanism. Furthermore, the export gate complex also has a sodium ion (Na<sup>+</sup>) channel to couple Na<sup>+</sup> influx with flagellar protein export. In this article, we review our current understanding of the activation mechanism of the dual-fuel protein export engine of the fT3SS. This review article is an extended version of a Japanese article, Membrane voltage-dependent activation of the transmembrane export gate complex in the bacterial flagellar type III secretion system, published in SEIBUTSU BUTSURI Vol. 62, p165–169 (2022).

**Key words:** ATPase, bacterial flagella, flagellar assembly, transmembrane ion channel, protein export, proton motive force, type III secretion system

**◀ Significance ▶**

The flagellar type III secretion system (fT3SS) consists of a transmembrane export gate complex powered by the electrochemical potential difference of protons across the cell membrane and an associated ATPase ring complex that serves as an activator of the export gate complex. The fT3SS is equipped with a dual-fuel engine that exploits H<sup>+</sup> and Na<sup>+</sup> as the coupling ions and a membrane voltage sensor to drive flagellar protein export, allowing the fT3SS to maintain its protein transport activity against various internal and external perturbations. This review describes our current understanding of the structure and function of the *Salmonella* fT3SS.

Corresponding author: Tohru Minamino, Graduate school of Frontier Biosciences, Osaka University, 1-3 Yamadaoka, Suita, Osaka 565-0871, Japan. ORCID iD: <https://orcid.org/0000-0002-8175-1951>, e-mail: [tohru@fbs.osaka-u.ac.jp](mailto:tohru@fbs.osaka-u.ac.jp)

## Introduction

The cell membrane is positively charged on the outside and negatively charged on the inside due to the difference in ion concentrations between the inside and outside of the cell, thereby creating the electric potential difference ( $\Delta\Psi$ ) across the cell membrane, which is defined as membrane voltage. Various membrane protein complexes, such as  $F_0F_1$ -ATP synthase, protein transporters, ion channels, ion-driven motility machines, and so on, utilize proton motive force (PMF), which consists of the  $\Delta\Psi$  and the proton ( $H^+$ ) concentration difference ( $\Delta pH$ ) across the cell membrane, to exert their biological activities. In physics,  $\Delta\Psi$  and  $\Delta pH$  are equivalent driving forces for  $H^+$  movement, and they are believed to play equivalent roles in biological functions as well, such as those involving membrane  $H^+$  channels [1]. However, the studies we describe here clearly indicate that  $\Delta\Psi$  and  $\Delta pH$  are used differently in the flagellar protein export process [2].

*Salmonella enterica* serovar Typhimurium (hereafter referred to as *Salmonella*) is a pathogenic bacterium that causes bacterial food poisoning, and *Salmonella* infection results in acute gastroenteritis. *Salmonella* cells use a long filamentous organelle called the flagellum to travel to intestinal epithelial cells of human body and then utilizes an appendage named the injectisome to directly inject virulence effector proteins into host cells for invasion. The flagellum also promotes bacterial adhesion to host cell surfaces and biofilm formation on solid surfaces. Thus, flagella-driven motility allows bacterial cells not only to reach a suitable site, but also to adhere efficiently to the cell surfaces for their invasion [3].

The *Salmonella* flagellum is composed of a basal body, a hook, and a filament (Figure 1). The basal body is embedded in the cell membranes and acts as a bi-directional rotary motor powered by PMF. The hook and filament extend outward from the cell body. The filament functions as a helical propeller to propel the cell body. The hook exists between the basal body and filament and works as a universal joint to transmit torque produced by the rotary motor to the helical propeller [4-6].

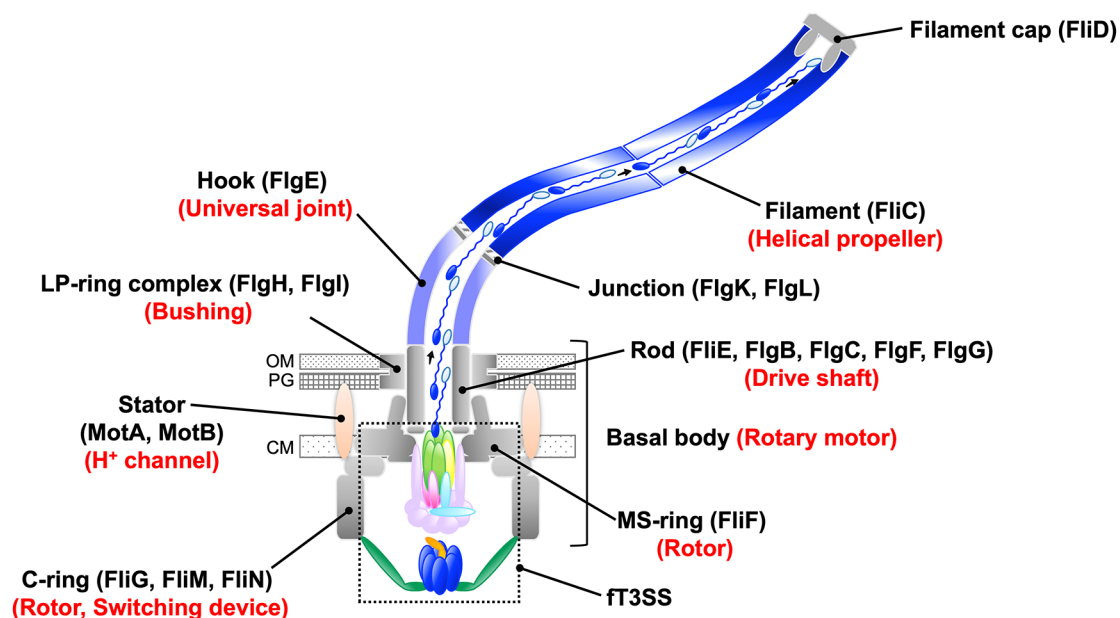


**Figure 1** Schematic diagram of the *Salmonella* flagellum. The bacterial flagellum consists of a basal body that acts as a bi-directional rotary motor, a filament that works as a helical propeller, and a hook that connects the basal body and filament and serves as a universal joint to transmit rotational force produced by the motor to the helical propeller. A dozen stator units surround the rotor ring complex consisting of the MS-ring and the C-ring. To construct the axial structure consisting of the rod, the hook, the junction, the filament, and the filament cap, each structural subunit is translocated by the flagellar type III secretion system (ft3SS), diffuses down the central channel and assembles at the distal end of the growing structure. OM, outer membrane; PG, peptidoglycan layer; CM, cytoplasmic membrane.

The *Salmonella* basal body consists of the C-ring (composed of FliG, FliM, FliN), the MS-ring (FliF), the P-ring (FlgI), the L-ring (FlgH) and the rod (FliE, FlgB, FlgC, FlgF, FlgG). These component proteins and their arrangement in the flagellum are highly conserved among bacterial species [7]. Recently, the entire structure of the *Salmonella* basal body has been revealed by cryoEM image analysis [8,9]. The MS-C-ring complex has 34-fold rotational symmetry and serves

as the rotor of the flagellar motor [10]. The C-ring also acts as a switching device to allow the motor to rotate in both counterclockwise and clockwise directions [11]. Maximally a dozen stator units surround the rotor, and each stator unit acts as a transmembrane  $H^+$  channel that couples  $H^+$  influx through the channel with torque generation [12]. The rod is a helical assembly consisting of 11 protofilaments that is straight and rigid against bending and twisting and acts as a drive shaft [13]. The P and L rings together form a very strong and stable ring complex that serves as a bushing for high-speed rod rotation inside it [14].

The basal body also contains a specific protein export apparatus required for construction of the axial structure consisting of the rod, the hook (FlgE), the hook-filament junction (FlgK, FlgL), the filament (FliC), and the filament cap (FliD) (Figure 1). Because the flagellar protein export apparatus is very similar in structure and function to the injectisome, they are categorized into the type III secretion system (T3SS) [15]. The T3SS is composed of a transmembrane export gate complex and a cytoplasmic ATPase ring complex (Figure 2) [16].

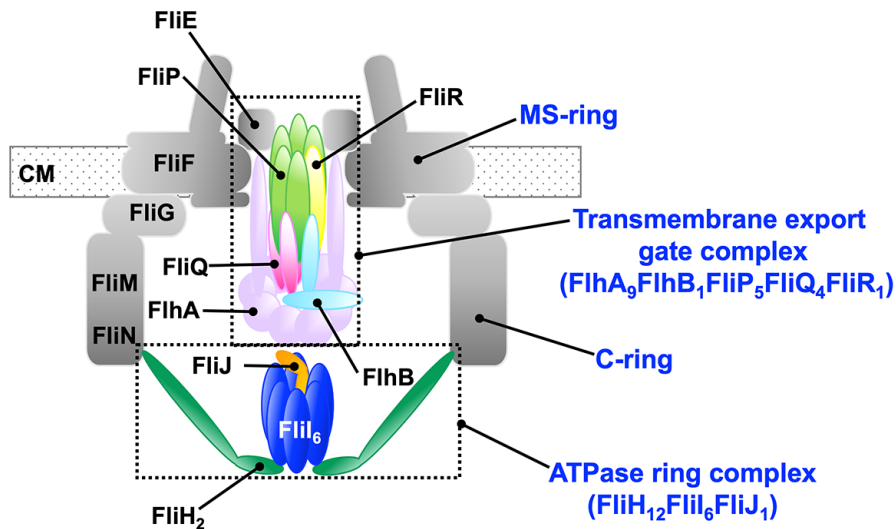


**Figure 2** Schematic diagram of the flagellar type III protein export apparatus. The flagellar protein export apparatus is composed of a transmembrane export gate complex with a stoichiometry of 9 FlhA, 1 FlhB, 5 FliP, 4 FliQ and 1 FliR and a cytoplasmic ATPase ring complex with a stoichiometry of 12 FliH, 6 FliI and 1 FliJ. The export gate complex is located within the MS-ring. The FliH dimer binds to each of 6 FliI subunits, and the interaction of the FliH dimer with FliI in the C-ring anchors the FliI<sub>6</sub>-FliJ ring to the base of the flagellum. CM, cytoplasmic membrane.

The transmembrane export gate complex of the *Salmonella* flagellar T3SS (ft3SS) is composed of 9 copies of FlhA, a single copy of FlhB, 5 copies of FliP, 4 copies of FliQ, and a single copy of FliR and is divided into two distinct structural parts: a transmembrane protein complex containing an ion channel and a polypeptide channel; and a docking platform for component proteins of the cytoplasmic ATPase complex, flagellar export chaperones, and export substrates [17-21]. The ion and polypeptide channels are located inside the MS-ring whereas the docking platform projects into the central cavity of the C-ring. The flagellar export gate complex is powered by PMF and serves as a  $H^+$ /protein antiporter that couples inward-directed  $H^+$  flow through the ion channel with outward-directed protein translocation through the polypeptide channel [2,22-24]. The export gate complex requires ATP hydrolysis by the cytoplasmic ATPase ring complex to become an efficient and robust  $H^+$ /protein antiporter under a variety of environmental conditions [2,25]. In addition to  $\Delta\Psi$ , the export gate complex by itself prefers to use sodium ions ( $Na^+$ ) to drive  $Na^+$ -coupled protein export over a wide range of external pH when the cytoplasmic ATPase complex is absent or non-functional [26,27]. Furthermore, when  $\Delta\Psi$  exceeds above a certain threshold value, an inactive export gate complex autonomously becomes an active  $H^+$ -driven protein transporter even in the absence of external  $Na^+$  [28]. These observations suggest that the export gate complex is equipped with a dual-fuel protein export engine and a membrane voltage sensor so that it can conduct both  $H^+$  and  $Na^+$  to drive ion-coupled protein export in a  $\Delta\Psi$ -dependent manner. Thus, the ft3SS can maintain its protein transport activity against internal and external perturbations. In this review article, we describe our current understanding of the activation mechanism of the dual-fuel export engine in the *Salmonella* ft3SS.

### FliP, FliQ, and FliR Form a Polypeptide Channel Inside the MS-ring

FliP and FliR assemble into the FliP<sub>5</sub>-FliR<sub>1</sub> complex with the help of FliO [29,30], and four FliQ subunits surround the

FliP<sub>5</sub>-FliR<sub>1</sub> complex to form the FliP<sub>5</sub>-FliQ<sub>4</sub>-FliR<sub>1</sub> complex [19] (Figure 3). The FliP<sub>5</sub>-FliQ<sub>4</sub>-FliR<sub>1</sub> complex is located within a central pore of the MS-ring and serves as a polypeptide channel for the translocation of export substrate across the cytoplasmic membrane. The structure of the FliP<sub>5</sub>-FliQ<sub>4</sub>-FliR<sub>1</sub> complex is formed with a helical array of subunits, and so FliE, which is the first export substrate transported by the  $\sigma^{54}$  [31], can directly assemble on FliP and FliR to form the most proximal part of the rod structure with a helical symmetry [8,9]. Interactions of FliE with FliP and FliR fully open the exit gate of the polypeptide channel, allowing other axial proteins to diffuse down the central channel of the growing structure and assemble at the distal end [32]. So, if FliE is missing in the basal body, the  $\sigma^{54}$  is unable to transport other axial proteins out of the cytoplasm [17,31].

### FlhB Regulates the Opening and Closing of the Polypeptide Channel

FlhB consists of an N-terminal transmembrane domain (FlhB<sub>TM</sub>) with four transmembrane helices (TMHs) and a C-terminal cytoplasmic domain (FlhB<sub>C</sub>) [33,34]. A single copy of FlhB directly associates with the FliP<sub>5</sub>-FliQ<sub>4</sub>-FliR<sub>1</sub> complex through interactions of FlhB<sub>TM</sub> with FliP, FliQ, and FliR (Figure 3) [20]. The cytoplasmic loop (FlhB<sub>Loop</sub>) between TMH-2 and TMH-3 wraps around the entrance gate of the polypeptide channel through the interactions with each FliQ subunit. FlhB<sub>C</sub> provides binding sites for export substrates such as the rod and hook proteins [35-37]. Recent genetic analysis has shown that FlhB<sub>C</sub>, together with the cytoplasmic ATPase complex, regulates the opening and closing of the entrance gate of the polypeptide channel [34].

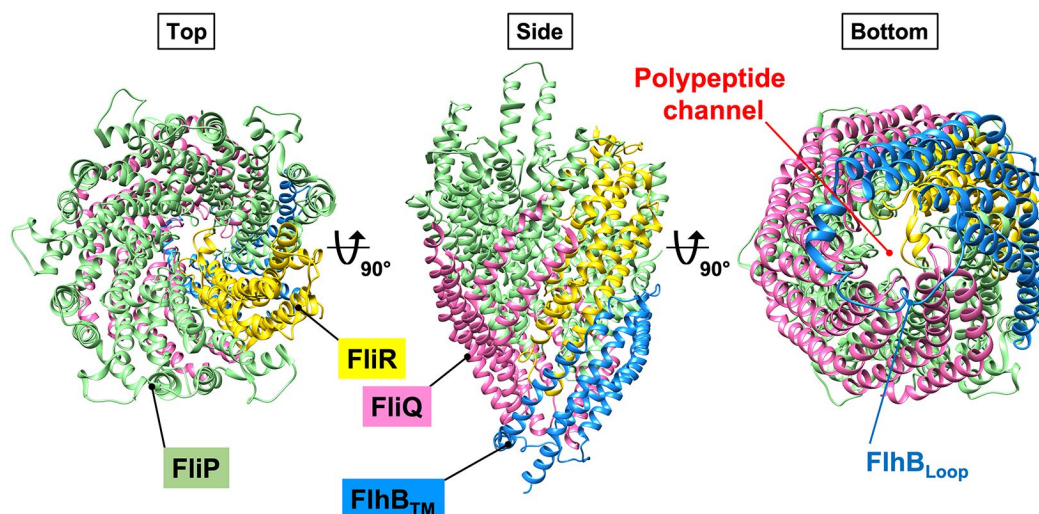


**Figure 3** CryoEM structure of the FlhB<sub>1</sub>-FliP<sub>5</sub>-FliQ<sub>4</sub>-FliR<sub>1</sub> complex [PDB ID: [6S3L](#)]. FliP (light green) and FliR (yellow) assemble into a helical structure with a stoichiometry of 5 FliP and 1 FliR molecules, and 4 FliQ (pink) molecules bind to the outside of the FliP<sub>5</sub>-FliR<sub>1</sub> complex, forming the FliP<sub>5</sub>-FliQ<sub>4</sub>-FliR<sub>1</sub> complex with a helical subunit array. The transmembrane domain of FlhB (light blue, FlhB<sub>TM</sub>) associates with the FliP<sub>5</sub>-FliQ<sub>4</sub>-FliR<sub>1</sub> complex. The central pore of the FliP<sub>5</sub>-FliQ<sub>4</sub>-FliR<sub>1</sub> complex serves as a polypeptide channel. The cytoplasmic loop of FlhB (FlhB<sub>Loop</sub>) encases all four FliQ molecules and seems to stabilize a closed conformation of the polypeptide channel.

The  $\sigma^{54}$  transports the hook protein during hook assembly. When the hook reaches its mature length of about 55 nm in *Salmonella*, the  $\sigma^{54}$  switches its substrate specificity from hook-type to filament-type, thereby terminating hook assembly and initiating filament assembly [38]. The  $\sigma^{54}$  infrequently secretes the FliK ruler protein during hook assembly to measure the hook length [39,40]. FliK is composed of an N-terminal domain (FliK<sub>N</sub>) that serves as a molecular ruler, a C-terminal domain (FliK<sub>C</sub>) that interacts with FlhB<sub>C</sub> to catalyze the substrate specificity switch, and a flexible linker region (FliK<sub>L</sub>) between FliK<sub>N</sub> and FliK<sub>C</sub> [41-43]. Recently, it has been reported that FliK<sub>L</sub> is required for efficient interaction of FliK<sub>C</sub> with FlhB<sub>C</sub> upon completion of hook assembly [44]. Thus, FlhB<sub>C</sub>, together with FliK, appears to bring the order to flagellar assembly.

### FlhA Provides a Docking Platform for Export Substrates and Flagellar Export Chaperones

FlhA is composed of an N-terminal transmembrane domain with eight TMHs, a C-terminal cytoplasmic domain (FlhA<sub>C</sub>) and a flexible linker (FlhA<sub>L</sub>) connecting these two domains [33,34,45]. FlhA interacts with FliP, FliQ, and FliR during

MS-ring formation, thereby assembling into a homo-nonameric ring structure [18,29,46-48]. High-speed atomic force microscopy has shown that FlhA<sub>C</sub> with the FlhA<sub>L</sub> linker can form a stable homo-nonameric ring *in vitro* whereas FlhA<sub>C</sub> without FlhA<sub>L</sub> cannot (Figure 4A), suggesting that FlhA<sub>L</sub> stabilizes the FlhA<sub>C</sub> ring structure [49]. This is well supported by the structure of the FlhA<sub>C</sub> ring revealed by cryoEM image analysis [21, PDB ID: [7AMY](#)]

The FlhA<sub>C</sub> ring structure serves as a docking platform for component proteins of the cytoplasmic ATPase complex, flagellar export chaperones, and export substrates and coordinates flagellar protein export with assembly in a highly organized and well-controlled manner, thereby the flagellar axial structure to be efficiently built on the cell surface [38]. The crystal structures of FlhA<sub>C</sub> show that it consists of domains D1, D2, D3, and D4 and adopts open [PDB ID: [3A5I](#)], semi-closed [PDB ID: [6AI0](#)], and closed [PDB ID: [3MYD](#)] conformations [50-52]. When FlhA<sub>C</sub> adopts the open conformation, there is a large cleft between domains D2 and D4. In contrast, when FlhA<sub>C</sub> switches its conformation from the open form to the closed form, domain D4 is much closer to domain D2 (Figure 4B). Molecular dynamic simulation has revealed that the *flhA(G368C/K548C)* mutation stabilizes a completely closed conformation at 300 K, thereby suppressing dynamic open-close domain motions and that the *flhA(F459C)* mutation restores cyclic open-close domain motions of FlhA<sub>C</sub> with the G368C/K548C substitution [53]. Because the *flhA(G368C/K548C)* mutation causes loss of motility in *Salmonella* whereas the *flhA(F459C)* mutation partially suppresses this motility defect [51], this suggests that the cyclic open-close domain motions of FlhA<sub>C</sub> are important for flagellar protein export by the ft3SS.

FlgN, FliS, and FliT function as flagellar export chaperones specific for FlgK/L, FliC, and FliD, respectively [4] and bind with high affinity to the highly conserved hydrophobic dimple of FlhA<sub>C</sub> formed by its Asp-456, Phe-459, and Thr-490 residues (Figure 4C), allowing the ft3SS to efficiently unfold and transport their cognate substrate to construct the flagellar filament at the tip of the hook [54-57]. These chaperones can bind to the open form of FlhA<sub>C</sub> but not to its closed form [51,58]. Because cyclic remodeling of hydrophobic side chain networks in FlhA<sub>C</sub> induces periodic open-close domain motions of FlhA<sub>C</sub> [53], such dynamic domain motions may facilitate the cycle of chaperone association and dissociation for efficient and robust protein transport during filament assembly.

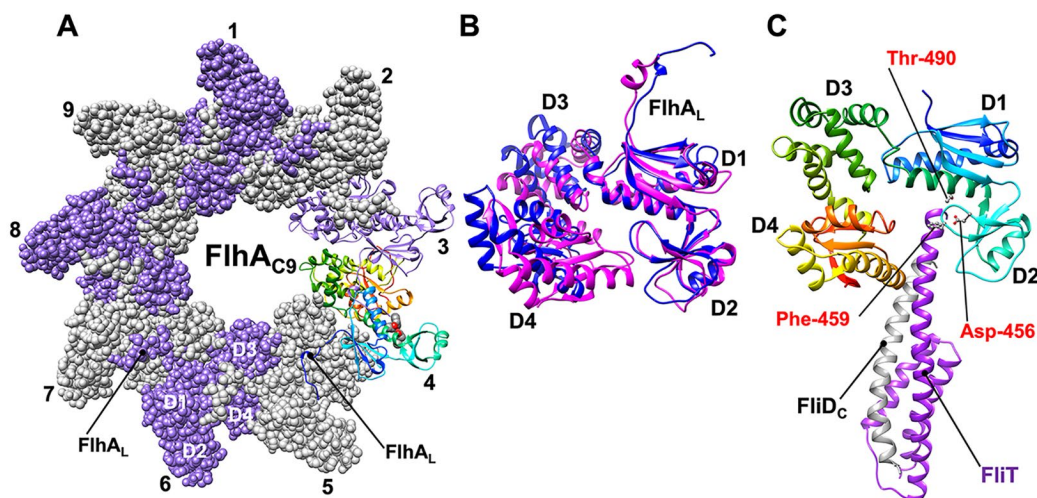


**Figure 4** Atomic model of the C-terminal cytoplasmic domain of FlhA (FlhA<sub>C</sub>). (A) End-on view of FlhA<sub>C</sub> nonameric ring structure. The FlhA<sub>C</sub> ring model is built by fitting domains D1 and D2 of FlhA<sub>C</sub> [PDB ID: [3A5I](#)] to those of MxiA<sub>C</sub> in the nonameric ring structure [PDB ID: [4A5P](#)]. The flexible linker region of FlhA (FlhA<sub>L</sub>) binds to its neighboring FlhA<sub>C</sub> subunit to stabilize the FlhA<sub>C</sub> ring structure. (B) Structural comparison between the open [blue, PDB ID: [3A5I](#)] and closed [magenta, PDB ID: [3MYD](#)] forms of FlhA<sub>C</sub>. When FlhA<sub>C</sub> adopts the closed form, domain D4 is much closer to domain D2. (C) The crystal structure of FlhA<sub>C</sub> in complex with the FliT-FliD chaperone-substrate complex [PDB ID: [6CH2](#)]. The FliT chaperone (purple) binds to the C-terminal segment of FliD (FliD<sub>C</sub>) to form the FliT-FliD complex. This complex binds to the well-conserved hydrophobic dimple at the interface between domains D1 and D2. Asp-456, Phe-459, and Thr-490 are critical for the FlhA<sub>C</sub>-FliT interaction.

### FlhA Acts as a Dual-fuel Export Engine of the ft3SS

In *Salmonella* wild-type cells,  $\Delta\Psi$  alone is sufficient for flagellar protein export by the transmembrane export gate complex over a wide range of environmental conditions [2,23,26]. In contrast, certain *Salmonella* mutants with FliI that cannot work as a flagellum-specific ATPase in the ft3SS require the  $\Delta pH$  component for flagellar protein export in

addition to the  $\Delta\Psi$  component [2]. This suggests that these two components of PMF plays distinct roles in the flagellar protein export process. Because the number and length of visible flagellar filaments produced by these mutant cells increase substantially with an increase in the extracellular  $\text{Na}^+$  concentration over a wide range of external pH (Figure 5) [26], the export gate complex has a dual-fuel export engine that can couple either  $\text{H}^+$  or  $\text{Na}^+$  flow with the translocation of export substrate through the polypeptide channel complex.

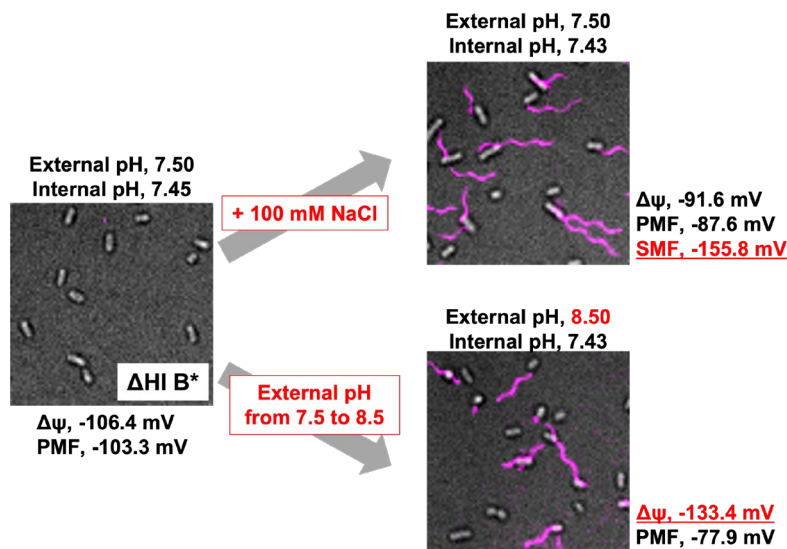


**Figure 5** Capability of the *Salmonella*  $\Delta fliH-fliI flhB(P28T)$  mutant to form flagella. The *Salmonella*  $\Delta fliH-fliI flhB(P28T)$  mutant ( $\Delta HI B^*$ ), which not only lacks both *fliH* and *fliI* genes, but also has the P28T substitution in FlhB, cannot form flagella when there is little difference between intracellular and extracellular proton concentrations (left panel). The  $\Delta HI B^*$  cells, however, can produce a few flagella in the presence of 100 mM NaCl (right, upper panel). An increase in  $\Delta\Psi$  generated by an upward shift of external pH from 7.5 to 8.5 also significantly increases the probability of filament formation by the  $\Delta HI B^*$  cells (right, bottom panel). PMF, proton motive force; SMF, sodium motive force. This figure is modified from ref. [59].

Which component of the export gate complex is responsible for the dual-fuel export engine? It has been shown that overexpression of *Salmonella* FlhA alone in *Escherichia coli* cells results in a significant decrease in intracellular pH [26]. Furthermore, overexpression of FlhA with the D208A substitution causes a further decrease in intracellular pH compared to wild-type FlhA. Because the D208A substitution exists in FlhA<sub>TM</sub>, these results suggest that FlhA<sub>TM</sub> has a  $\text{H}^+$  channel activity and that Asp-208, which is highly conserved among FlhA homologs, suppresses massive  $\text{H}^+$  flow through the FlhA<sub>TM</sub> channel. Interestingly, the intracellular  $\text{Na}^+$  concentration of *E. coli* cells overexpressing *Salmonella* FlhA has been shown to increase to about 100 mM by adding 100 mM NaCl to the culture medium, indicating that FlhA<sub>TM</sub> also has the  $\text{Na}^+$  channel activity. However, the  $\text{Na}^+$  channel activity of FlhA with the D208A substitution is essentially the same as that of the wild-type, indicating that Asp-208 of FlhA is not involved in the  $\text{Na}^+$  influx through the  $\text{Na}^+$  channel. Therefore, it seems likely that FlhA<sub>TM</sub> is the one that serves as a dual-fuel export engine of the ft3SS.

### FlgN Chaperone Activates the $\text{Na}^+$ -driven Export Engine

The *Salmonella*  $\Delta fliH-fliI flhB(P28T)$  mutant, which not only lacks both *fliH* and *fliI* genes encoding components of the cytoplasmic ATPase ring complex, but also contains the *flhB(P28T)* point mutation, has been shown to preferentially use sodium motive force (SMF) across the cytoplasmic membrane to produce a few flagella over a wide range of external pH (Figure 5) [26]. In contrast, when FliH and FliI are co-expressed from a plasmid, the  $\Delta fliH-fliI flhB(P28T)$  mutant can transport flagellar proteins to produce flagella even in the absence of external  $\text{Na}^+$  [26]. Furthermore, removal of  $\text{Na}^+$  from the culture medium has no effect on the export of flagellar proteins by *Salmonella* wild-type cells [26]. These observations suggest that the export gate complex prefers to use the  $\text{H}^+$ -driven export engine when the cytoplasmic ATPase complex is fully functional whereas it prefers to use the  $\text{Na}^+$ -driven export engine when the ATPase complex is absent or non-functional. Thus, the  $\text{Na}^+$ -driven export engine appears to serve as a backup engine for the ft3SS.

How does the  $\text{Na}^+$  channel of FlhA<sub>TM</sub> open to become active when the ATPase ring complex ceases to function? FliJ, which is a component of the cytoplasmic ATPase ring complex, binds to FlhA<sub>L</sub> with high affinity and FlhA<sub>C</sub> with low affinity [60]. When FliJ cannot stably bind to FlhA<sub>L</sub>, the export gate complex opens the  $\text{Na}^+$  channel of FlhA<sub>TM</sub> to drive

Na<sup>+</sup>-coupled protein export [27]. Removal of FlgN from the  $\Delta fliH-fliI flhB(P28T)$  mutant causes a completely non-motile phenotype because none of the flagellar proteins are transported out of the cytoplasm even in the presence of 100 mM NaCl [27], indicating that FlgN is required for Na<sup>+</sup>-coupled protein export by the export gate complex. Interestingly, either of two mutations in FlhA<sub>C</sub>, *flhA(D456V)* to *flhA(T490M)*, significantly suppresses this motility defect [27], suggesting that these two mutations allow FlhA<sub>C</sub> to adopt a conformation mimicking a FlgN-bound state to let the export gate complex utilize Na<sup>+</sup> as the coupling ion to transport flagellar proteins in the absence of FlgN. Because FlgN alone can bind to FlhA<sub>C</sub> with nanomolar affinity [55], the FlgN-FlhA<sub>C</sub> interaction appear to generate a conformational change in FlhA<sub>TM</sub> that activate its Na<sup>+</sup> channel function. Thus, FlgN serves not only as an export chaperone specific for FlgK and FlgL, but also as a switch that turns on the Na<sup>+</sup>-driven export engine when the cytoplasmic ATPase ring complex becomes non-functional (Figure 6, middle panel).

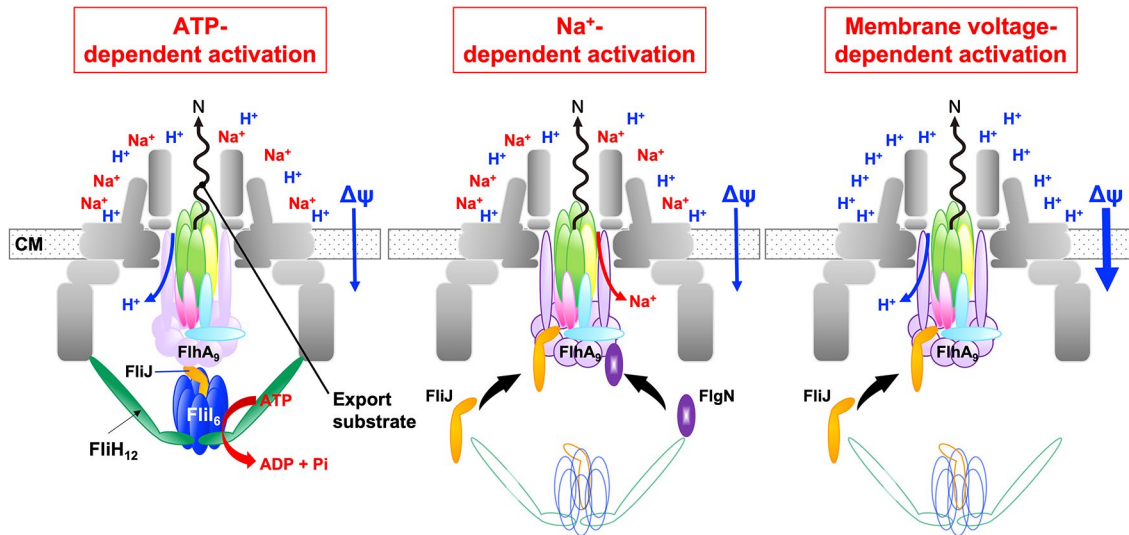


**Figure 6** Activation mechanism of the dual-fuel export engine in the ft3SS. When the cytoplasmic ATPase complex is functional, ATP hydrolysis by the FliI ATPase activates the export gate complex to become an active protein transporter through an interaction between FliJ and FlhA. As a result, the export gate complex efficiently utilizes  $\Delta\Psi$  or PMF to couple H<sup>+</sup> flow through the FlhA ion channel with the translocation of export substrate into the polypeptide channel (left panel). When the cytoplasmic ATPase ring complex becomes non-functional, FlgN binds to FlhA and activates the Na<sup>+</sup> channel of FlhA, allowing the export gate complex to drive Na<sup>+</sup>-coupled protein export (middle panel). Furthermore, an increase in  $\Delta\Psi$  above a certain threshold value stabilizes the interaction between FliJ and FlhA, and this interaction activates the H<sup>+</sup> channel of FlhA, allowing the export gate complex to drive H<sup>+</sup>-coupled protein export in the absence of external Na<sup>+</sup> (right panel). Thus, the export gate complex is equipped with a dual-fuel export engine and a membrane voltage sensor. CM, cytoplasmic membrane. This figure is modified from ref. 59.

### The Export Gate Complex is Equipped with a Membrane Voltage Sensor

How does the export gate complex utilize  $\Delta\Psi$ , which is measured as membrane voltage, to drive ion-coupled protein export. Intracellular pH of bacterial cells is unaffected by changes in external pH and is generally maintained at around 7.5. So, to maintain total PMF as much as possible, the cells autonomously increase  $\Delta\Psi$  when external pH is higher than 7.5 [61-63]. In fact, an upward shift of external pH from 7.5 to 8.5 increases  $\Delta\Psi$  significantly but decreases the total PMF in *Salmonella* cells (Figure 5). Even in the absence of external Na<sup>+</sup>, the transmembrane export gate complex of the  $\Delta fliH-fliI flhB(P28T)$  mutant can become an active H<sup>+</sup>/protein antiporter to drive H<sup>+</sup>-coupled protein export when  $\Delta\Psi$  exceeds a certain threshold value [28]. As a result, many  $\Delta fliH-fliI flhB(P28T)$  mutant cells produce a few flagella even in the absence of external Na<sup>+</sup> (Figure 5). These observations suggest that the export gate complex is equipped with a voltage-gated mechanism to activate H<sup>+</sup>-coupled protein export.

At what stage of the flagellar protein export process is  $\Delta\Psi$  used? Overexpression of FliJ significantly increases the secretion level of flagellar proteins by the *Salmonella*  $\Delta fliH-fliI flhB(P28T)$  mutant at an external pH value of 7.5, and an upward shift of external pH from 7.5 to 8.5 does not enhance flagellar protein export by this mutant [28]. Furthermore, removal of FliJ from the  $\Delta fliH-fliI flhB(P28T)$  mutant significantly reduces the  $\Delta\Psi$ -dependent protein export activity of the export gate complex even at an external pH value of 8.5, but the *flhA(T490M)* mutation located in FlhA<sub>C</sub> significantly restores this protein export activity in the absence of FliJ [28]. Because FliJ binds to FlhA<sub>L</sub> to facilitate H<sup>+</sup>-coupled protein

export by the export gate complex [2,64], FlhA itself seems to have a membrane voltage-dependent activation mechanism, and an increase in  $\Delta\Psi$  above a certain threshold value may stabilize the interaction between FlhA<sub>L</sub> and FliJ, thereby opening the H<sup>+</sup> channel of FlhA<sub>TM</sub> to facilitate H<sup>+</sup> flow to be coupled with flagellar protein export (Figure 6, right panel). Therefore,  $\Delta\Psi$  appears to be necessary not only for an efficient and robust interaction between FlhA<sub>L</sub> and FliJ, but also for efficient H<sup>+</sup> influx through the FlhA<sub>TM</sub> ion channel to be coupled with flagellar protein export.

### The Cytoplasmic ATPase Ring Complex Serves as an Activator of the Export Engine

The cytoplasmic ATPase ring complex is composed of 12 copies of FliH, 6 copies of FliI, and 1 copy of FliJ and serves as an activator of the transmembrane export gate complex (Figure 7) [65]. FliI is a Walker-type ATPase [66] and forms a homo-hexameric ring to hydrolyze ATP at the interface between FliI subunits [67,68]. The entire structure of FliI is very similar to the  $\alpha$  and  $\beta$  subunits of F<sub>0</sub>F<sub>1</sub> ATP synthase, which couples H<sup>+</sup> flow through the F<sub>0</sub> part with ATP synthesis by the F<sub>1</sub> part [69]. The FliI ring has been observed to be located in the cytoplasmic side of the flagellar basal body C-ring by electron cryotomography and sub-tomogram averaging [70].

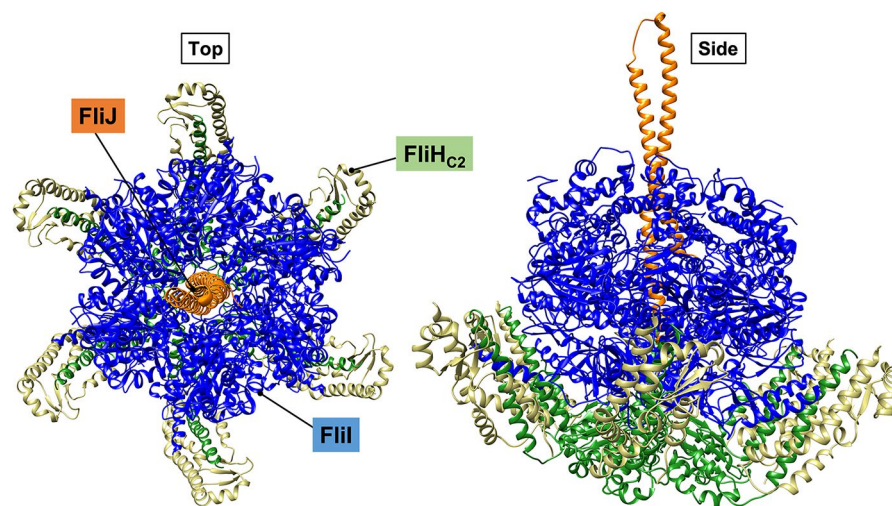


**Figure 7** Atomic model of the FliH<sub>C12</sub>-FliI<sub>6</sub>-FliJ<sub>1</sub> ring complex. The FliH<sub>C2</sub>-FliI<sub>1</sub> complex [FliI; PDB ID: [5B0Q](#)] and FliJ [PDB ID: [3AJW](#)] are shown in C $\alpha$  ribbon representation. FliI assembles into a homo-hexameric ring. The C-terminal domain of FliH (FliH<sub>C</sub>) forms a homodimer through its central coiled coil structure, and the FliH<sub>C</sub> dimer (FliH<sub>C2</sub>) binds to each N-terminal domain of the FliI<sub>6</sub> ring. FliJ binds to the central pore of the FliI<sub>6</sub> ring.

The FliI<sub>6</sub> ring requires FliH for efficient localization to the flagellar base [71-73]. FliH adopts a quite elongated conformation and forms a homodimer through its central  $\alpha$ -helical coiled coil structure [74,75]. The C-terminal domain of FliH (FliH<sub>C</sub>) shows different conformations from each other in the two subunits of the dimer structure [76]. These two FliH<sub>C</sub> domains bind to different regions of the N-terminal domain of FliI (FliI<sub>N</sub>), and these two distinct interactions are demonstrated to be critical for the stable formation of the FliH<sub>2</sub>-FliI complex [76,77] (Figure 7). Two highly conserved Trp-7 and Trp-10 residues in the N-terminal domain of FliH (FliH<sub>N</sub>) are directly involved in the interactions with FliI<sub>N</sub> in the C-ring for FliI ring location and FlhA in the export gate complex for export substrate shuttle function of the FliH<sub>2</sub>-FliI complex [78,79]. High-resolution single-molecule imaging techniques have shown that these two distinct interactions are necessary for FliI by labelling FliI with a yellow fluorescent protein to efficiently localize it at the base of the flagellum [80]. Because FliH<sub>N</sub> and FliH<sub>C</sub> are homologous to the b and  $\delta$  subunits of F<sub>0</sub>F<sub>1</sub> ATP synthase, respectively, which form the peripheral stalk connecting the cytoplasmic F<sub>1</sub> unit to the membrane-embedded F<sub>0</sub> unit [81], FliH is likely to act as a peripheral stalk to stably anchor the cytoplasmic FliI<sub>6</sub> ring to the flagellar base through interactions of FliH with FliI<sub>N</sub>, FliI<sub>N</sub>, and FlhA.

FliJ adopts an antiparallel coiled-coil structure that is structurally similar to the two-stranded  $\alpha$ -helical coiled-coil part of the  $\gamma$  subunit of F<sub>0</sub>F<sub>1</sub> ATP synthase and binds to the central pore of the FliI<sub>6</sub> ring [82] (Figure 7). This is supported by the cryoEM structure of the ATPase ring complex of the virulence associated T3SS, consisting of 6 copies of the FliI homolog SctN and a single copy of the FliJ homolog SctO [83].

How does the cytoplasmic ATPase ring complex activate the H<sup>+</sup>-driven export engine? FliJ requires FliH and FliI for efficient binding to FlhA<sub>L</sub>, thereby turning on the H<sup>+</sup>-driven export engine in the ft3SS [2]. A highly conserved Glu-211 residue in the catalytically active site of FliI is directly involved in the ATP hydrolysis reaction cycle [25,68]. The ATPase

activity of FliI with the E211D substitution is about 100-fold lower than that of wild-type FliI. However, the number and length of flagellar filaments produced by more than 90% of the *fliI(E211D)* mutant cells are reduced to only about half of those of the wild type [25], indicating that infrequent ATP hydrolysis by FliI with the E211D substitution is sufficient for processive protein transport by the FT3SS. This suggests that the rate of ATP hydrolysis by the FliI ATPase is not at all coupled with the export rate by the FT3SS and that ATP consumption by the FT3SS must be relatively low during flagellar assembly. Interestingly, the *fliI(E211Q)* mutant whose substitution does not affect ATP binding to the catalytic site of FliI but completely inhibit ATP hydrolysis [68] produces flagella albeit at a very low probability [25], suggesting that even just the binding of ATP to the catalytic site of FliI can activate the export gate complex to some degree. Thus, the energy derived from the binding of ATP to FliI and the subsequent ATP hydrolysis by the FliI<sub>6</sub> ring seems to be used only to activate the export gate complex (Figure 6, left panel).

## Conclusions and Perspective

The transmembrane export gate complex is composed of a dual-fuel protein export engine that uses either H<sup>+</sup> or Na<sup>+</sup> as the coupling ion to drive ion-driven protein export, a polypeptide channel, a membrane voltage sensor, and a substrate docking platform. Based on available information, three distinct gate activation mechanisms have been proposed (Figure 6). The transmembrane export gate complex remains inactive until the cytoplasmic ATPase ring complex is installed into the flagellar base. ATP hydrolysis by the FliI ATPase induces conformational changes in the FlhA<sub>TM</sub> domain through an interaction between FliJ and FlhA<sub>L</sub>, opening the H<sup>+</sup> channel of FlhA<sub>TM</sub> and unlocking the entrance gate of the polypeptide channel. As a result, the transmembrane export gate complex can act as a H<sup>+</sup>/protein antiporter that efficiently utilizes  $\Delta\Psi$  to drive H<sup>+</sup>-coupled protein export in a highly processive manner (left panel). When FliJ cannot efficiently bind to FlhA<sub>L</sub>, the FlgN chaperone binds to FlhA<sub>C</sub> and activates the Na<sup>+</sup> channel of FlhA<sub>TM</sub> to facilitate Na<sup>+</sup> influx to be coupled with flagellar protein export (middle panel). The export gate complex is also equipped with a voltage-gated mechanism, in which an increase in  $\Delta\Psi$  above a certain threshold value significantly stabilizes the FliJ-FlhA<sub>L</sub> interaction in the absence of FliH and FliI, thereby activating the H<sup>+</sup> channel of FlhA<sub>TM</sub> to a considerable degree. As a result, the export gate complex can drive H<sup>+</sup>-coupled protein export (right panel).

Recently, the entire structure of the FliP<sub>5</sub>-FliQ<sub>4</sub>-FliR<sub>1</sub> polypeptide channel complex associated with the basal body has been revealed by cryoEM image analysis [8,9]. However, because both FlhA and FlhB are missing in these cryoEM structures, it remains unknown how H<sup>+</sup> and Na<sup>+</sup> with different ionic radii move through the ion channel of FlhA<sub>TM</sub>, how ATP hydrolysis by the cytoplasmic ATPase ring complex activates only the H<sup>+</sup> channel of FlhA<sub>TM</sub>, how the FlgN chaperone opens only the Na<sup>+</sup> channel of FlhA<sub>TM</sub>, how the H<sup>+</sup> channel of FlhA<sub>TM</sub> is activated in a  $\Delta\Psi$ -dependent manner, and how the export gate complex couples ion flow through the ion channel with the translocation of export substrate through the polypeptide channel. To clarify these critical questions, the overall structure of FlhA in complex with the FlhB<sub>1</sub>-FliP<sub>5</sub>-FliQ<sub>4</sub>-FliR<sub>1</sub> complex is needed to be revealed by high-resolution cryoEM image analysis.

## Conflict of Interest

The authors declare no conflicts of interest

## Author Contributions

T.M., M.K., Y.V.M., and K.N. wrote the manuscript

## Acknowledgements

This work was supported in part by JSPS KAKENHI Grant Numbers JP19H03182, JP22H02573, and JP22K19274 (to T.M.), JP20K15749 and JP22K06162 (to M.K.), and JP18K06159, JP21H05532 and JP21K06099 (to Y.V.M.) and JST PRESTO Grant Number JPMJPR204B (to Y.V.M.). This work has also been supported by Platform Project for Supporting Drug Discovery and Life Science Research (BINDS) from AMED under Grant Number JP21am0101117 and JP22ama121003 to K.N., by the Cyclic Innovation for Clinical Empowerment (CiCLE) from AMED under Grant Number JP17pc0101020 to K.N. and by JEOL YOKOGUSHI Research Alliance Laboratories of Osaka University to K.N.

## References

- [1] Nicholls, D. G., Ferguson, S. J. Bioenergetics 4 (Academic Press, London, 2013).
- [2] Minamino, T., Morimoto, Y. V., Hara, N., Namba, K. An energy transduction mechanism used in bacterial flagellar type III protein export. Nat. Commun. 2, 475 (2011). <https://doi.org/10.1038/ncomms1488>

- [3] Erhardt, M. Strategies to block bacterial pathogenesis by interference with motility and chemotaxis. *Curr. Top Microbiol. Immunol.* 398, 185-205 (2016). [https://doi.org/10.1007/82\\_2016\\_493](https://doi.org/10.1007/82_2016_493)
- [4] Minamino, T., Namba, K. Self-assembly and type III protein export of the bacterial flagellum. *J. Mol. Microbiol. Biotechnol.* 7, 5-17 (2004). <https://doi.org/10.1159/000077865>
- [5] Morimoto, Y. V., Minamino, T. Structure and function of the bi-directional bacterial flagellar motor. *Biomolecules* 4, 217-234 (2014). <https://doi.org/10.3390/biom4010217>
- [6] Nakamura, S., Minamino, T. Flagella-driven motility of bacteria. *Biomolecules* 9, 279 (2019). <https://doi.org/10.3390/biom9070279>
- [7] Minamino, T., Imada, K. The bacterial flagellar motor and its structural diversity. *Trends Microbiol.* 23, 267-274 (2015). <https://doi.org/10.1016/j.tim.2014.12.011>
- [8] Johnson, S., Furlong, E. J., Deme, J. C., Nord, A. L., Caesar, J. J. E., Chevance, F. F. V., et al. Molecular structure of the intact bacterial flagellar basal body. *Nat Microbiol.* 6, 712-721 (2021). <https://doi.org/10.1038/s41564-021-00895-y>
- [9] Tan, J., Zhang, X., Wang, X., Xu, C., Chang, S., Wu, H., et al. Structural basis of assembly and torque transmission of the bacterial flagellar motor. *Cell* 184, 2665-2679 e19 (2021). <https://doi.org/10.1016/j.cell.2021.03.057>
- [10] Kawamoto, A., Miyata, T., Makino, F., Kinoshita, M., Minamino, T., Imada, K., et al. Native flagellar MS ring is formed by 34 subunits with 23-fold and 11-fold subsymmetries. *Nat. Commun.* 12, 4223 (2021). <https://doi.org/10.1038/s41467-021-24507-9>
- [11] Minamino, T., Kinoshita, M., Namba, K. Directional switching mechanism of the bacterial flagellar motor. *Comput. Struct. Biotechnol. J.* 17, 1075-1081 (2019). <https://doi.org/10.1016/j.csbj.2019.07.020>
- [12] Minamino, T., Terahara, N., Kojima, S., Namba, K. Autonomous control mechanism of stator assembly in the bacterial flagellar motor in response to changes in the environment. *Mol. Microbiol.* 109, 723-734 (2018). <https://doi.org/10.1111/mmi.14092>
- [13] Fujii, T., Kato, T., Hiraoka, K. D., Miyata, T., Minamino, T., Chevance, F. F., et al. Identical folds used for distinct mechanical functions of the bacterial flagellar rod and hook. *Nat. Commun.* 8, 14276 (2017). <https://doi.org/10.1038/ncomms14276>
- [14] Yamaguchi, T., Makino, F., Miyata, T., Minamino, T., Kato, T., Namba, K. Structure of the molecular bushing of the bacterial flagellar motor. *Nat. Commun.* 12, 4469 (2021). <https://doi.org/10.1038/s41467-021-24715-3>
- [15] Wagner, S., Diepold, A. A unified nomenclature for injectisome-type type III secretion systems. *Curr. Top Microbiol. Immunol.* 427, 1-10 (2020). [https://doi.org/10.1007/82\\_2020\\_210](https://doi.org/10.1007/82_2020_210)
- [16] Minamino, T., Kawamoto, A., Kinoshita, M., Namba, K. Molecular organization and assembly of the export apparatus of flagellar type III secretion systems. *Curr. Top Microbiol. Immunol.* 91-107 (2019). [https://doi.org/10.1007/82\\_2019\\_170](https://doi.org/10.1007/82_2019_170)
- [17] Minamino, T., Macnab, R. M. Components of the *Salmonella* flagellar export apparatus and classification of export substrates. *J. Bacteriol.* 181, 1388-1394 (1999). <https://doi.org/10.1128/JB.181.5.1388-1394.1999>
- [18] Abrusci, P., Vergara-Irigaray, M., Johnson, S., Beeby, M. D., Hendrixson, D. R., Roversi, P., et al. Architecture of the major component of the type III secretion system export apparatus. *Nat. Struct. Mol. Biol.* 20, 99-104 (2013). <https://doi.org/10.1038/nsmb.2452>
- [19] Kuhlen, L., Abrusci, P., Johnson, S., Gault, J., Deme, J., Caesar, J., et al. Structure of the core of the type III secretion system export apparatus. *Nat. Struct. Mol. Biol.* 25, 583-590 (2018). <https://doi.org/10.1038/s41594-018-0086-9>
- [20] Kuhlen, L., Johnson, S., Zeitler, A., Baurle, S., Deme, J. C., Caesar, J. J. E., et al. The substrate specificity switch FlhB assembles onto the export gate to regulate type three secretion. *Nat. Commun.* 11, 1296 (2020). <https://doi.org/10.1038/s41467-020-15071-9>
- [21] Kuhlen, L., Johnson, S., Cao, J., Deme, J. C., Lea, S. M. Nonameric structures of the cytoplasmic domain of FlhA and SctV in the context of the full-length protein. *PLoS One* 16, e0252800 (2021). <https://doi.org/10.1371/journal.pone.0252800>
- [22] Minamino, T., Namba, K. Distinct roles of the FliI ATPase and proton motive force in bacterial flagellar protein export. *Nature* 451, 485-488 (2008). <https://doi.org/10.1038/nature06449>
- [23] Paul, K., Erhardt, M., Hirano, T., Blair, D. F., Hughes, K. T. Energy source of flagellar type III secretion. *Nature* 451, 489-492 (2008). <https://doi.org/10.1038/nature06497>
- [24] Morimoto, Y. V., Kami-Ike, N., Miyata, T., Kawamoto, A., Kato, T., Namba, K., et al. High-resolution pH imaging of living bacterial cells to detect local pH differences. *mBio* 7, e01911-16 (2016). <https://doi.org/10.1128/mBio.01911-16>
- [25] Minamino, T., Morimoto, Y. V., Kinoshita, M., Aldridge, P. D., Namba, K. The bacterial flagellar protein export apparatus processively transports flagellar proteins even with extremely infrequent ATP hydrolysis. *Sci. Rep.* 4, 7579 (2014). <https://doi.org/10.1038/srep07579>

- [26] Minamino, T., Morimoto, Y. V., Hara, N., Aldridge, P. D., Namba, K. The bacterial flagellar type III export gate complex is a dual fuel engine that can use both H<sup>+</sup> and Na<sup>+</sup> for flagellar protein export. *PLoS Pathog.* 12, e1005495 (2016). <https://doi.org/10.1371/journal.ppat.1005495>
- [27] Minamino, T., Kinoshita, M., Morimoto, Y. V., Namba, K. The FlgN chaperone activates the Na<sup>+</sup>-driven engine of the *Salmonella* flagellar protein export apparatus. *Commun Biol* 4, 335 (2021). <https://doi.org/10.1038/s42003-021-01865-0>
- [28] Minamino, T., Morimoto, Y. V., Kinoshita, M., Namba, K. Membrane voltage-dependent activation mechanism of the bacterial flagellar protein export apparatus. *Proc. Natl. Acad. Sci. U.S.A.* 118, e2026587118 (2021). <https://doi.org/10.1073/pnas.2026587118>
- [29] Fukumura, T., Makino, F., Dietsche, T., Kinoshita, M., Kato, T., Wagner, S., et al. Assembly and stoichiometry of the core structure of the bacterial flagellar type III export gate complex. *PLoS Biol.* 15, e2002281 (2017). <https://doi.org/10.1371/journal.pbio.2002281>
- [30] Fabiani, F. D., Renault, T. T., Peters, B., Dietsche, T., Galvez, E. J. C., Guse, A., et al. A flagellum-specific chaperone facilitates assembly of the core type III export apparatus of the bacterial flagellum. *PLoS Biol.* 15, e2002267 (2017). <https://doi.org/10.1371/journal.pbio.2002267>
- [31] Minamino, T., Yamaguchi, S., Macnab, R. M. Interaction between FliE and FlgB, a proximal rod component of the flagellar basal body of *Salmonella*. *J. Bacteriol.* 182, 3029-3036. (2000). <https://doi.org/10.1128/JB.182.11.3029-3036.2000>
- [32] Hendriksen, J. J., Lee, H. J., Bradshaw, A. J., Namba, K., Chevance, F. F. V., Minamino, T., et al. Genetic analysis of the *Salmonella* FliE protein that forms the base of the flagellar axial structure. *mBio* 12, e0239221 (2021). <https://doi.org/10.1128/mBio.02392-21>
- [33] Minamino, T., Iino, T., Kutuskake, K. Molecular characterization of the *Salmonella typhimurium* *flhB* operon and its protein products. *J. Bacteriol.* 176, 7630-7637 (1994). <https://doi.org/10.1128/jb.176.24.7630-7637.1994>
- [34] Kinoshita, M., Namba, K., Minamino, T. A positive charge region of *Salmonella* FliI is required for ATPase formation and efficient flagellar protein export. *Commun. Biol.* 4, 464 (2021). <https://doi.org/10.1038/s42003-021-01980-y>
- [35] Minamino, T., Macnab, R. M. Domain structure of *Salmonella* FlhB, a flagellar export component responsible for substrate specificity switching. *J. Bacteriol.* 182, 4906-4914 (2000). <https://doi.org/10.1128/JB.182.17.4906-4914.2000>
- [36] Evans, L. D., Poulter, S., Terentjev, E. M., Hughes, C., Fraser, G. M. A chain mechanism for flagellum growth. *Nature* 504, 287-290 (2013). <https://doi.org/10.1038/nature12682>
- [37] Qu, D., Jiang, M., Duffin, C., Hughes, K. T., Chevance, F. F. V. Targeting early proximal-rod component substrate FlgB to FlhB for flagellar-type III secretion in *Salmonella*. *PLoS Genet.* 18, e1010313 (2022). <https://doi.org/10.1371/journal.pgen.1010313>
- [38] Minamino, T. Hierarchical protein export mechanism of the bacterial flagellar type III protein export apparatus. *FEMS Microbiol. Lett.* 365, fny117 (2018). <https://doi.org/10.1093/femsle/fny117>
- [39] Minamino, T., Gonzalez-Pedrajo, B., Yamaguchi, K., Aizawa, S. I., Macnab, R. M. FliK, the protein responsible for flagellar hook length control in *Salmonella*, is exported during hook assembly. *Mol. Microbiol.* 34, 295-304 (1999). <https://doi.org/10.1046/j.1365-2958.1999.01597.x>
- [40] Erhardt, M., Singer, H. M., Wee, D. H., Keener, J. P., Hughes, K. T. An infrequent molecular ruler controls flagellar hook length in *Salmonella enterica*. *EMBO J.* 30, 2948-2961 (2011). <https://doi.org/10.1038/emboj.2011.185>
- [41] Shibata, S., Takahashi, N., Chevance, F. F., Karlinsey, J. E., Hughes, K. T., Aizawa, S. FliK regulates flagellar hook length as an internal ruler. *Mol. Microbiol.* 64, 1404-1415 (2007). <https://doi.org/10.1111/j.1365-2958.2007.05750.x>
- [42] Minamino, T., Ferris, H. U., Moriya, N., Kihara, M., Namba, K. Two parts of the T3S4 domain of the hook-length control protein FliK are essential for the substrate specificity switching of the flagellar type III export apparatus. *J. Mol. Biol.* 362, 1148-1158 (2006). <https://doi.org/10.1016/j.jmb.2006.08.004>
- [43] Kinoshita, M., Aizawa, S. I., Inoue, Y., Namba, K., Minamino, T. The role of intrinsically disordered C-terminal region of FliK in substrate specificity switching of the bacterial flagellar type III export apparatus. *Mol. Microbiol.* 105, 572-588 (2017). <https://doi.org/10.1111/mmi.13718>
- [44] Kinoshita, M., Tanaka, S., Inoue, Y., Namba, K., Aizawa, S. I., Minamino, T. The flexible linker of the secreted FliK ruler is required for export switching of the flagellar protein export apparatus. *Sci. Rep.* 10, 838 (2020). <https://doi.org/10.1038/s41598-020-57782-5>
- [45] Saijo-Hamano, Y., Minamino, T., Macnab, R. M., Namba, K. Structural and functional analysis of the C-terminal cytoplasmic domain of FlhA, an integral membrane component of the type III flagellar protein export apparatus in *Salmonella*. *J. Mol. Biol.* 343, 457-466 (2004). <https://doi.org/10.1016/j.jmb.2004.08.067>
- [46] Kihara, M., Minamino, T., Yamaguchi, S., Macnab, R. M. Intergenic suppression between the flagellar MS ring

- protein FliF of *Salmonella* and FlhA, a membrane component of its export apparatus. *J. Bacteriol.* 183, 1655-1662 (2001). <https://doi.org/10.1128/JB.183.5.1655-1662.2001>
- [47] Kawamoto, A., Morimoto, Y. V., Miyata, T., Minamino, T., Hughes, K. T., Kato, T., et al. Common and distinct structural features of *Salmonella* injectisome and flagellar basal body. *Sci. Rep.* 3, 3369 (2013). <https://doi.org/10.1038/srep03369>
- [48] Morimoto, Y. V., Ito, M., Hiraoka, K. D., Che, Y. S., Bai, F., Kami-Ike, N., et al. Assembly and stoichiometry of FliF and FlhA in *Salmonella* flagellar basal body. *Mol. Microbiol.* 91, 1214-1226 (2014). <https://doi.org/10.1111/mmi.12529>
- [49] Terahara, N., Inoue, Y., Kodera, N., Morimoto, Y. V., Uchihashi, T., Imada, K., et al. Insight into structural remodeling of the FlhA ring responsible for bacterial flagellar type III protein export. *Sci. Adv.* 4, eaao7054 (2018). <https://doi.org/10.1126/sciadv.aao7054>
- [50] Saijo-Hamano, Y., Imada, K., Minamino, T., Kihara, M., Shimada, M., Kitao, A., et al. Structure of the cytoplasmic domain of FlhA and implication for flagellar type III protein export. *Mol. Microbiol.* 76, 260-268 (2010). <https://doi.org/10.1111/j.1365-2958.2010.07097.x>
- [51] Inoue, Y., Ogawa, Y., Kinoshita, M., Terahara, N., Shimada, M., Kodera, N., et al. Structural insights into the substrate specificity switch mechanism of the type III protein export apparatus. *Structure* 27, 965-976 (2019). <https://doi.org/10.1016/j.str.2019.03.017>
- [52] Moore, S. A., Jia, Y. Structure of the cytoplasmic domain of the flagellar secretion apparatus component FlhA from *Helicobacter pylori*. *J. Biol. Chem.* 285, 21060-21069 (2010). <https://doi.org/10.1074/jbc.M110.119412>
- [53] Minamino, T., Kinoshita, M., Inoue, Y., Kitao, A., Namba, K. Conserved GYXLI motif of FlhA is involved in dynamic domain motions of FlhA required for flagellar protein export. *Microbiol. Spectr.* 10, e0111022 (2022). <https://doi.org/10.1128/spectrum.01110-22>
- [54] Minamino, T., Kinoshita, M., Hara, N., Takeuchi, S., Hida, A., Koya, S., et al. Interaction of a bacterial flagellar chaperone FlgN with FlhA is required for efficient export of its cognate substrates. *Mol. Microbiol.* 83, 775-788 (2012). <https://doi.org/10.1111/j.1365-2958.2011.07964.x>
- [55] Kinoshita, M., Hara, N., Imada, K., Namba, K., Minamino, T. Interactions of bacterial flagellar chaperone-substrate complexes with FlhA contribute to co-ordinating assembly of the flagellar filament. *Mol. Microbiol.* 90, 1249-1261 (2013). <https://doi.org/10.1111/mmi.12430>
- [56] Furukawa, Y., Inoue, Y., Sakaguchi, A., Mori, Y., Fukumura, T., Miyata, T., et al. Structural stability of flagellin subunit affects the rate of flagellin export in the absence of FliS chaperone. *Mol. Microbiol.* 102, 405-416 (2016). <https://doi.org/10.1111/mmi.13469>
- [57] Minamino, T., Morimoto, Y. V., Kinoshita, M., Namba, K. Multiple roles of flagellar export chaperones for efficient and robust flagellar filament formation in *Salmonella*. *Front Microbiol.* 12, 756044 (2021). <https://doi.org/10.3389/fmicb.2021.756044>
- [58] Xing, Q., Shi, K., Portaliou, A., Rossi, P., Economou, A., Kalodimos, C. G. Structures of chaperone-substrate complexes docked onto the export gate in a type III secretion system. *Nat. Commun.* 9, 1773 (2018). <https://doi.org/10.1038/s41467-018-04137-4>
- [59] Minamino, T., Kinoshita, M., Morimoto, Y. V., Namba, K. Membrane voltage-dependent activation of the transmembrane export gate complex in the bacterial flagellar type III secretion system. *SEIBUTSU BUTSURI* 62, 165-169 (2022). <https://doi.org/10.2142/biophys.62.165>
- [60] Inoue, Y., Kinoshita, M., Kida, M., Takekawa, N., Namba, K., Imada, K., et al. The FlhA linker mediates flagellar protein export switching during flagellar assembly. *Commun. Biol.* 4, 646 (2021). <https://doi.org/10.1038/s42003-021-02177-z>
- [61] Nakamura, S., Kami-ike, N., Yokota, J. P., Kudo, S., Minamino, T., Namba, K. Effect of intracellular pH on the torque-speed relationship of bacterial proton-driven flagellar motor. *J. Mol. Biol.* 386, 332-338 (2009). <https://doi.org/10.1016/j.jmb.2008.12.034>
- [62] Krulwich, T. A., Sachs, G., Padan, E. Molecular aspects of bacterial pH sensing and homeostasis. *Nat. Rev. Microbiol.* 9, 330-343 (2011). <https://doi.org/10.1038/nrmicro2549>
- [63] Prindle, A., Liu, J., Asally, M., Ly, S., Garcia-Ojalvo, J., Suel, G. M. Ion channels enable electrical communication in bacterial communities. *Nature* 527, 59-63 (2015). <https://doi.org/10.1038/nature15709>
- [64] Ibuki, T., Uchida, Y., Hironaka, Y., Namba, K., Imada, K., Minamino, T. Interaction between FliJ and FlhA, components of the bacterial flagellar type III export apparatus. *J. Bacteriol.* 195, 466-473 (2013). <https://doi.org/10.1128/JB.01711-12>
- [65] Minamino, T., Kinoshita, M., Namba, K. Insight Into distinct functional roles of the flagellar ATPase complex for flagellar assembly in *Salmonella*. *Front Microbiol.* 13, 864178 (2022). <https://doi.org/10.3389/fmicb.2022.864178>
- [66] Fan, F., Macnab, R. M. Enzymatic characterization of FliI. An ATPase involved in flagellar assembly in *Salmonella typhimurium*. *J. Biol. Chem.* 271, 31981-31988 (1996). <https://doi.org/10.1074/jbc.271.50.31981>

- [67] Claret, L., Calder, S. R., Higgins, M., Hughes, C. Oligomerization and activation of the FliI ATPase central to bacterial flagellum assembly. *Mol. Microbiol.* 48, 1349-1355 (2003). <https://doi.org/10.1046/j.1365-2958.2003.03506.x>
- [68] Kazetani, K., Minamino, T., Miyata, T., Kato, T., Namba, K. ATP-induced FliI hexamerization facilitates bacterial flagellar protein export. *Biochem. Biophys. Res. Commun.* 388, 323-327 (2009). <https://doi.org/10.1016/j.bbrc.2009.08.004>
- [69] Imada, K., Minamino, T., Tahara, A., Namba, K. Structural similarity between the flagellar type III ATPase FliI and F1-ATPase subunits. *Proc. Natl. Acad. Sci. U.S.A.* 104, 485-490 (2007). <https://doi.org/10.1073/pnas.0608090104>
- [70] Chen, S., Beeby, M., Murphy, G. E., Leadbetter, J. R., Hendrixson, D. R., Briegel, A., et al. Structural diversity of bacterial flagellar motors. *EMBO J.* 30, 2972-2981 (2011). <https://doi.org/10.1038/emboj.2011.186>
- [71] Gonzalez-Pedrajo, B., Minamino, T., Kihara, M., Namba, K. Interactions between C ring proteins and export apparatus components: a possible mechanism for facilitating type III protein export. *Mol. Microbiol.* 60, 984-998 (2006). <https://doi.org/10.1111/j.1365-2958.2006.05149.x>
- [72] McMurry, J. L., Murphy, J. W., Gonzalez-Pedrajo, B. The FliN-FliH interaction mediates localization of flagellar export ATPase FliI to the C ring complex. *Biochemistry* 45, 11790-11798 (2006). <https://doi.org/10.1021/bi0605890>
- [73] Paul, K., Harmon, J. G., Blair, D. F. Mutational analysis of the flagellar rotor protein FliN: identification of surfaces important for flagellar assembly and switching. *J. Bacteriol.* 188, 5240-5248 (2006). <https://doi.org/10.1128/JB.00110-06>
- [74] Minamino, T., Macnab, R. M. FliH, a soluble component of the type III flagellar export apparatus of *Salmonella*, forms a complex with FliI and inhibits its ATPase activity. *Mol. Microbiol.* 37, 1494-1503 (2000). <https://doi.org/10.1046/j.1365-2958.2000.02106.x>
- [75] Gonzalez-Pedrajo, B., Fraser, G. M., Minamino, T., Macnab, R. M. Molecular dissection of *Salmonella* FliH, a regulator of the ATPase FliI and the type III flagellar protein export pathway. *Mol. Microbiol.* 45, 967-982 (2002). <https://doi.org/10.1046/j.1365-2958.2002.03047.x>
- [76] Imada, K., Minamino, T., Uchida, Y., Kinoshita, M., Namba, K. Insight into the flagella type III export revealed by the complex structure of the type III ATPase and its regulator. *Proc. Natl. Acad. Sci. U.S.A.* 113, 3633-3638 (2016). <https://doi.org/10.1073/pnas.1524025113>
- [77] Minamino, T., Gonzalez-Pedrajo, B., Oosawa, K., Namba, K., Macnab, R. M. Structural properties of FliH, an ATPase regulatory component of the *Salmonella* type III flagellar export apparatus. *J. Mol. Biol.* 322, 281-290 (2002). [https://doi.org/10.1016/s0022-2836\(02\)00754-4](https://doi.org/10.1016/s0022-2836(02)00754-4)
- [78] Minamino, T., Yoshimura, S. D., Morimoto, Y. V., Gonzalez-Pedrajo, B., Kami-Ike, N., Namba, K. Roles of the extreme N-terminal region of FliH for efficient localization of the FliH-FliI complex to the bacterial flagellar type III export apparatus. *Mol. Microbiol.* 74, 1471-1483 (2009). <https://doi.org/10.1111/j.1365-2958.2009.06946.x>
- [79] Hara, N., Morimoto, Y. V., Kawamoto, A., Namba, K., Minamino, T. Interaction of the extreme N-terminal region of FliH with FlhA is required for efficient bacterial flagellar protein export. *J. Bacteriol.* 194, 5353-5360 (2012). <https://doi.org/10.1128/JB.01028-12>
- [80] Bai, F., Morimoto, Y. V., Yoshimura, S. D., Hara, N., Kami-Ike, N., Namba, K., et al. Assembly dynamics and the roles of FliI ATPase of the bacterial flagellar export apparatus. *Sci. Rep.* 4, 6528 (2014). <https://doi.org/10.1038/srep06528>
- [81] Pallen, M. J., Bailey, C. M., Beatson, S. A. Evolutionary links between FliH/YscL-like proteins from bacterial type III secretion systems and second-stalk components of the FoF1 and vacuolar ATPases. *Protein Sci.* 15, 935-941 (2006). <https://doi.org/10.1110/ps.051958806>
- [82] Ibuki, T., Imada, K., Minamino, T., Kato, T., Miyata, T., Namba, K. Common architecture of the flagellar type III protein export apparatus and F- and V-type ATPases. *Nat. Struct. Mol. Biol.* 18, 277-282 (2011). <https://doi.org/10.1038/nsmb.1977>
- [83] Majewski, D. D., Worrall, L. J., Hong, C., Atkinson, C. E., Vuckovic, M., Watanabe, N., et al. Cryo-EM structure of the homohexameric T3SS ATPase-central stalk complex reveals rotary ATPase-like asymmetry. *Nat. Commun.* 10, 626 (2019). <https://doi.org/10.1038/s41467-019-08477-7>